# Cooperative Dimerization of a Heterocyclic Diamidine Determines Sequence-Specific DNA Recognition†

Farial Tanious,‡ W. David Wilson,*,‡ Lei Wang,‡ Arvind Kumar,‡ David W. Boykin,*,‡ Carine Marty,§ Brigitte Baldeyrou,§ and Christian Bailly*,§

*Department of Chemistry and Laboratory for Chemical and Biological Sciences, Georgia State University, Atlanta, Georgia 30303, and INSERM U-524 et Laboratoire de Pharmacologie Antitumorale du Centre Oscar Lambret, IRCL, Place de Verdun, 59045 Lille, France*

*Received May 21, 2003; Revised Manuscript Received September 21, 2003*

ABSTRACT: In the course of a program aimed at discovering novel DNA-targeted antiparasitic drugs, the phenylfuran−benzimidazole unfused aromatic dication DB293 was identified as the first diamidine capable of forming stacked dimers in the DNA minor groove of GC-containing sequences. Its preferred binding sequence encompasses the tetranucleotide 5′-ATGA·5′-TCAT to which DB293 binds tightly with a strong positive cooperativity. Here we have investigated the influence of the DNA sequence on drug binding using two complementary technical approaches: surface plasmon resonance and DNase I footprinting. The central dinucleotide of the primary ATGA motif was systematically varied to represent all of the eight possible combinations (AXGA and ATYA, where X or Y = A, T, G, or C). Binding affinities for each site were precisely measured by SPR, and the extent of cooperative drug binding was also determined. The sequence recognition process was found to be extremely dependent on the nature of the central dinucleotide pair. Modification of the central TG step decreases binding affinity by a factor varying from 2 to over 500 depending on the base substitution. However, the diminished binding affinity does not affect the unique binding mode. In nearly all cases, the SPR titrations revealed a positive cooperativity in complex formation which reflects the ease of the dication to form stacked dimeric motifs in the DNA minor groove. DNase I footprinting served to identify additional binding sites for DB293 in the context of long DNA sequences offering a large variety of randomly distributed or specifically designed sites. The ATGA motif provided the best receptor for the drug, but lower affinity sequences were also identified. The design of two DNA fragments composed of various targeted tetranucleotide binding sites separated by an "insulator" (nonbinding) sequence allowed us to delineate further the influence of DNA sequence on drug binding and to identify a novel high-affinity site: 5′-ACAA·5′-TTGT. Collectively, the SPR and footprinting results show that the consensus sequence 5′-(A/T)-TG-(A/T) represents the optimal site for cooperative dimerization of the heterocyclic diamidine DB293.

The concept of inhibiting gene expression with DNA targeted small molecules developed from studies initiated more than 30 years ago when the pyrrole amidine antibiotics netropsin and distamycin were found to bind selectively to AT-rich DNA sequences (*1*, *2*). This discovery leads to the design of sequence-selective netropsin-derived molecules, later christened lexitropsins, which extragenetically read the base sequences from the minor groove of double-stranded DNA (*3*). Later on, hairpin polyamides emerged as an extremely potent class of lexitropsin-derived gene silencing tools (*4*, *5*), and this strategy has generated some encouraging results at the biological level (*6*−*8*). However, despite the recognized ability of hairpin polyamides to modify gene expression in cultured cells (*9*, *10*), clinical applications of these molecules have not emerged. The poor nuclear uptake capacities of these compounds may limit their development as therapeutic agents (*11*, *12*).

Furamidine and related diamidine dications represent another prominent class of DNA minor groove binders with promising clinical values (*13*). Several compounds of this type have revealed potent antiparasitic activities against the pathogen *Pneumocystis carinii* (*14*−*18*) and other parasites (*19*−*21*), and an amidoxime prodrug of furamidine (*22*) is in advanced phase II clinical trials as an antitrypanosomal drug and is projected to enter phase III trials in the next year. The prodrug also shows exceptional oral activities against *Plasmodium falciparum* and other African trypanosome species (*13*). Evidence has been accumulated that these compounds exert their antiparasitic activities via DNA recognition and possibly interference with DNA binding proteins (*23*, *24*).

In the course of a collaborative structure−activity program aimed at designing sequence-selective DNA minor groove binders, we have previously discovered the phenylfuran−

† This work was supported by grants from the National Institutes of Health (Research Grant GM 61587 to W.D.W. and D.W.B.) and from the Ligue Nationale Contre le Cancer (Equipe labellisée la Ligue) (to C.B.). The BIAcore 2000 instrumentation was purchased through funds from the Georgia Research Alliance.

* To whom correspondence should be addressed. E-mail: bailly@lille.inserm.fr.

‡ Georgia State University.

§ INSERM U-524.

10.1021/bi034852y CCC: $25.00 
Published on Web 10/31/2003

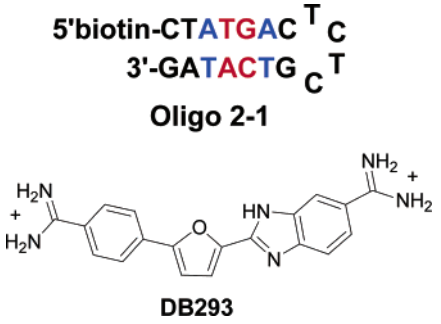


FIGURE 1: DB293 and oligo 2-1 sequence. Stem sequences for all variations at the TG positions of oligo 2-1 are shown in Table 1.

benzimidazole dication DB293 (Figure 1) which shows an exceptional capacity to form antiparallel dimers stacking within the DNA minor groove to recognize GC-containing sequences (*25*). This is the first proposal for a new mechanism of small molecule−DNA recognition since the discovery of the distamycin dimer (*26*, *27*), and we are pursuing detailed studies of the complex. Our initial studies have shown that the binding of DB293 to its favored binding site, 5′-ATGA (*28*), is highly cooperative and strictly dependent on the compound structure. Slight changes of the phenylfuran−benzimidazole core altering the stacking properties of the diamidine can abolish totally the capacity to recognize GC-containing sequences (*29*). The tight binding of DB293 to ATGA sites relies on specific complementarity between the drug dimers and the DNA minor groove surface at the particular binding sites, but solvation of the target sites and hydrophobic interactions also play a role in determining the strength of the drug−DNA association (*30*).

The reason the drug forms dimers under certain circumstances remains unclear, and the molecular rules that govern the DB293−ATGA recognition process are not precisely known. Two strategies have been devised to better define this interaction. The first one consists of determining how specific variations of the drug structure affect the DNA recognition properties (*28*, *29*). The second one, reported here, uses modifications of the nucleotide sequence of the bioreceptor to study the possible interactions between DB293 and a variety of potential binding sites. In the first case where the drug is varied, it is possible to discover novel dimer-forming compounds. In the second case, we wish to identify other binding sequences. The two complementary approaches, modulating either the ligand or its receptor, provide essential information that allows us to dissect the molecular mechanism by which DB293 recognizes its preferred sequences.

Here we have investigated the binding of DB293 to a range of DNA sequences encompassing the site ATGA and/or variations of this tetranucleotide sequence. The key questions we wish to address are the following: (1) How do the modifications of the preferred ATGA site affect the extent of binding of DB293? (2) Are there other high-affinity sites apart from ATGA? (3) Does the drug bind as a monomer or as a dimer to the modified sites? (4) When dimer formation is observed, are there specific drug−drug interactions that facilitate recognition? A dual strategy based on the methods of DNase I footprinting and surface plasmon resonance (SPR)[1] detection of binding to DNA oligomers was employed to address these issues of *affinity*, *selectivity*, *stoichiometry*, and *cooperativity*. With a high molecular mass sensitivity (in the order of 200 in current instruments), SPR is well suited to determine whether DB293 binds as a monomer or a dimer to a particular site, and the use of a range of oligonucleotide sequences allows for an estimation of the binding level at each designed target sequence (*31*). On the other hand, the DNase I footprinting methodology is widely appreciated to identify short binding sites within a long DNA sequence, and the use of a combinatorial-type set of appropriately designed sequences allows for the selection and ranking of different binding sites. Quantitative footprinting has become popular to evaluate the relative binding affinities of a given drug for a series of binding sequences (*32*, *33*). By examining how well the results correlate between two techniques of SPR and footprinting which provide complementary information on binding (*34*), we can make some assessment of this efficient combined strategy. The work reported here provides useful guidelines for the design of novel DNA reading drugs with potential direct therapeutic action and/or biotechnology applications.

## MATERIALS AND METHODS

*Compound.* The synthesis of compound DB293 has been reported previously (*16*).

*Immobilization of DNA and Biosensor−Surface Plasmon Resonance (SPR) Binding Studies.* Samples of 5′-biotin-labeled hairpin DNA duplexes from Midland Certified Reagent Co. (HPLC purified and desalted) in MES10 buffer [0.01 M MES [2-(*N*-morpholino)ethanesulfonic acid], 0.001 M ethylenediaminetetraacetic acid (EDTA), and 0.1 M NaCl with the pH adjusted to 6.25 with NaOH solution] at 50 nM concentration were applied to flow cells in streptavidin-derivatized sensor chips (BIAcore SA) by direct flow at 5 $\mu$L/min in BIAcore 2000 or 3000 SPR instruments as previously described (*28*). Nearly the same amount of all oligomers was immobilized on each flow cell to facilitate comparisons of binding. Three flow cells were used to immobilize DNA oligomer samples, and the fourth cell was left blank as a control. Steady-state binding analysis was performed with multiple injections of different compound concentrations over the immobilized DNA surface at a flow rate in MES10 buffer at 25 °C (*29*). Termination of sample injection was followed by buffer flow to allow evaluation of the dissociation process. The diamidine compounds dissociated from the DNA complex in buffer flow alone, and no special surface regeneration was required. Binding results from the SPR experiments were fit with either a single-site model ($K_2 = 0$) or a two-site model:

$$r = \mathrm{RU}/\mathrm{RU}_{max} = (K_1C_{free} + 2K_1K_2C_{free}^2)/(1 + K_1C_{free} + 2K_1K_2C_{free}^2) \quad (1)$$

where $r$ represents the moles of bound compound per mole of DNA hairpin duplex, $K_1$ and $K_2$ are macroscopic binding constants, $C_{free}$ is the free compound concentration in equilibrium with the complex, and $\mathrm{RU}_{max}$ is the RU value for binding a single compound to the immobilized oligomer (*35*). The free compound concentration is fixed by the concentration in the flow solution.

[1] Abbreviations: bp, base pair; RU, response unit; SPR, surface plasmon resonance; TBE, Tris−borate−EDTA.

*Purification of DNA Restriction Fragments and Radiolabeling.* The different plasmids were isolated from *Escherichia coli* by a standard sodium dodecyl sulfate−sodium hydroxide lysis procedure and purified by banding in CsCl−ethidium bromide gradients. The two 198-bp fragments were obtained from plasmids pMS1 and pMS2 (kindly provided by Professor K. R. Fox, University of Southampton) (*36*) after digestion with the restriction enzymes *Hin*dIII and *Xba*I followed by 3′-$^{32}$P-end-labeling at the *Hin*dIII site with [α-$^{32}$P]dATP (Amersham, 3000 Ci/mmol) and AMV reverse transcriptase (Roche). To clone the 319 base pair duplexes A and B containing selected variants of the ATGA motif, a synthetic 63-mer oligonucleotide and its complement were mixed at a 1:1 ratio, heated to 90 °C for 5 min, and slowly cooled to form the duplex. The sequences of the oligonucleotides were designed so that they could be cloned between the *Eco*RI and *Bam*HI sites of the pBSK vector. The vector plasmid pBSK was double digested with *Bam*HI and *Eco*RI prior to ligation with the insert. The resulting plasmid construct was transformed into *E. coli* cells (*Epicurian coli* SURE2 competent cells, Stratagene). The 319-bp duplexes A and B for footprinting were prepared by 3′-$^{32}$P-end-labeling of the *Eco*RI−*Pvu*II double digest of the plasmids using [α-$^{32}$P]dATP and AMV reverse transcriptase. In all cases, the labeled digestion products were separated on a 6% polyacrylamide gel under nondenaturing conditions in TBE buffer (89 mM Tris−borate, pH 8.3, 1 mM EDTA). After autoradiography, the requisite band of DNA was excised, crushed, and soaked in water overnight at 37 °C. This suspension was filtered through a Millipore 0.22 μm filter, and the DNA was precipitated with ethanol. Following washing with 70% ethanol and vacuum-drying of the precipitate, the labeled DNA was resuspended in 10 mM Tris adjusted to pH 7.0 containing 10 mM NaCl.

*DNase I Footprinting.* Bovine pancreatic deoxyribonuclease I (DNase I; Sigma Chemical Co.) was stored as a 7200 unit/mL solution in 20 mM NaCl, 2 mM $MgCl_2$, and 2 mM $MnCl_2$, pH 8.0. The stock solutions of DNase I was kept at −20 °C and freshly diluted to the desired concentration immediately prior to use. Footprinting experiments were performed essentially as previously described (*37*). Briefly, reactions were conducted in a total volume of 10 μL. Samples (3 μL) of the labeled DNA fragments were incubated with 5 μL of the buffered solution containing the ligand at the appropriate concentration. After 30 min incubation at 37 °C to ensure equilibration of the binding reaction, the digestion was initiated by the addition of 2 μL of a DNase I solution whose concentration was adjusted to yield a final enzyme concentration of about 0.01 unit/mL in the reaction mixture. The reaction was stopped by freeze-drying after 3 min. Samples were lyophilized and resuspended in 5 μL of an 80% formamide solution containing tracking dyes. The DNA samples were then heated at 90 °C for 4 min and chilled in ice for 4 min prior to electrophoresis.

*Electrophoresis and Quantitation by Storage Phosphorimaging.* DNA cleavage products were resolved by polyacrylamide gel electrophoresis under denaturating conditions (0.3 mm thick, 8% acrylamide containing 8 M urea). After electrophoresis (about 2.5 h at 60 W, 1600 V, in Tris−borate−EDTA-buffered solution; BRL sequencer model S2), gels were soaked in 10% acetic acid for 10 min, transferred to Whatman 3MM paper, and dried under vacuum at 80 °C. A Molecular Dynamics 425E phosphorimager was used to collect data from the storage screens exposed to dried gels overnight at room temperature. Baseline-corrected scans were analyzed by integrating all of the densities between two selected boundaries using ImageQuant (version 3.3) software. Each resolved band was assigned to a particular bond within the DNA fragments by comparison of its position relative to sequencing standards generated by treatment of the DNA with dimethyl sulfate followed by piperidine-induced cleavage at the modified guanine bases in DNA (G-track).

Table 1: BIAcore Binding Results[a]

| sequence | $K_1K_2$ (×10$^{13}$), M$^{-2}$ | $K_1$ (×10$^6$), M$^{-1}$ | $K_2$ (×10$^6$), M$^{-1}$ |
|---|---|---|---|
| CTATGAC | 16.0 | 2.6 | 62 |
| CTATAAC | 7.1 | 3.4 | 21 |
| CTATTAC | 3.8 | 9.8 | 3.9 |
| CTATCAC | 3.6 | 2.6 | 14 |
| CTAGGAC | 0.1 | 0.27 | 3.6 |
| CTAAGAC | 0.7 | 1.4 | 5.1 |
| CTACGAC | 0.03 | 0.15 | 2.1 |

[a] All of the BIAcore experiments were conducted in MES buffer with 0.1 M NaCl added at 25 °C. All of the DNA sequences only show the stem part of the hairpin sequence in the BIAcore experiment with the hairpin loop TCTC for all of the DNAs. The individual errors in $K_1$ and $K_2$ are about twice those in the product due to correlation between the two $K$ values. A slight increase in $K_1$ can be somewhat compensated by a slight decrease in $K_2$ to give a product that is relatively constant and fits the data points within experimental error.

## RESULTS

*Biosensor−SPR: BIAcore.* To evaluate the affinity of DB293 for short, specific DNA sequences at high resolution, we have conducted biosensor−SPR experiments with a series of DNA samples (sequences given in Table 1) immobilized on a biosensor surface as described in Materials and Methods. Our initial experiments used oligo 2-1 with an ATGA binding site (Figure 1). This sequence was defined by footprinting experiments with DB293 and clearly illustrates the strong and unusual binding of DB293 to a GC-containing sequence. Two important additional features of the interaction of DB293 with the ATGA sequence of Figure 1 are the maximum value for the RU response as saturation is approached ($RU_{max}$) and the cooperativity of the interaction. The RU values depend on the mass of DB293 bound to the immobilized DNA, and thus the maximum RU value is directly related to the stoichiometry of the complex of DB293 with each sequence. We have previously shown that the RU maximum of DB293 with sequences such as ATGA that bind the compound as a cooperative dimer is twice the value observed with sequences such as AATT where it binds as a more classical minor groove 1:1 complex (*29*). Positive cooperativity in complex formation is another characteristic feature of the formation of stacked dimer complexes with DNA. Positive cooperativity is defined by a $K_2$ value that is greater than $K_1$. From statistical factors, $K_2$ is predicted to be only 0.25 times $K_1$ for noncooperative interactions at equivalent binding sites, and a $K_2 > K_1$ indicates significant positive cooperativity in binding. The primary observation in support of the dimeric binding mode is the sigmoidal shape of the binding curves that suggests cooperative interactions.

Our earlier experiments illustrated the critical importance of an ATGA recognition sequence for stacked dimer forma-

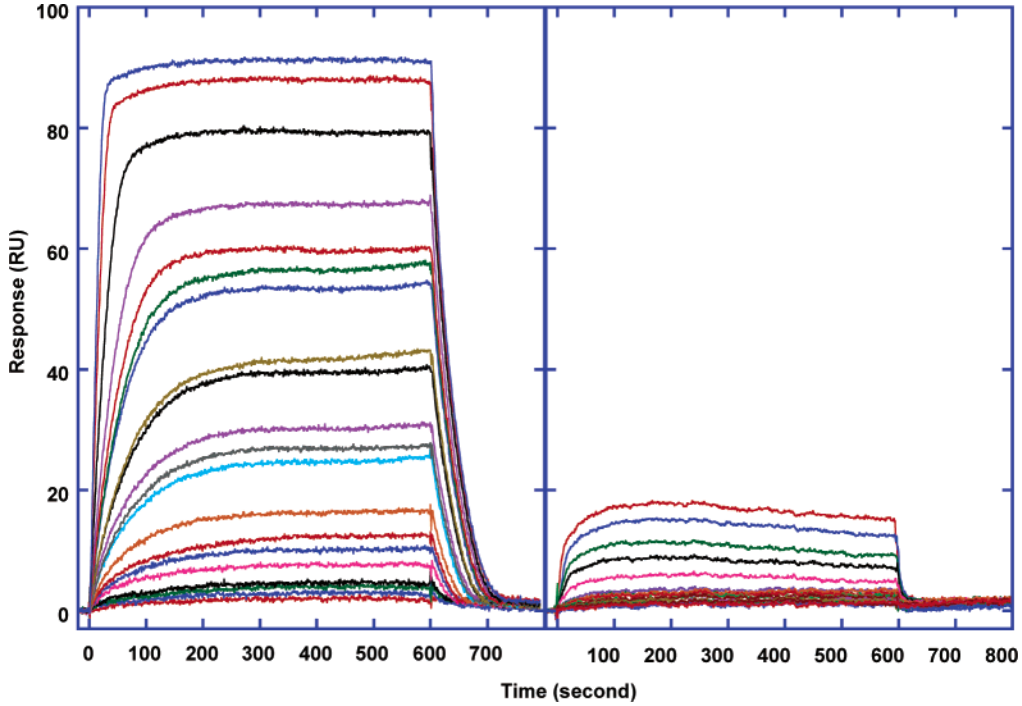


FIGURE 2: Sensorgrams for binding of DB293 to the ATGA (left) and ACGA (right) immobilized DNA hairpin oligomer sequences in MES10 buffer at 25 °C. In both plots the DB293 concentration increases from 0 (bottom of the plots) to $4 \times 10^{-7}$ M (top curve in both plots). As can be seen for this concentration range, much more DB293 is bound to the ATGA than to the ACGA sequence.

tion (*28*). Flanking sequence effects were found to be much less important for dimer formation. To probe the effects of variations in the ATGA sequence in more detail, oligomers were used in which the central TG was systematically changed to all other possible base pair combinations. The original ATGA sequence is used as a control, and this gives a total of seven different oligomer sequences for BIAcore analysis with DB293 (Figure 1). BIAcore sensorgrams for DB293 binding to the sequences ATGA and ACGA are shown for reference in Figure 2. Direct binding plots of the RU response at steady state from sensorgrams such as those in Figure 2 are shown in Figure 3 for DB293 binding to ATGA, AAGA, ATTA, and AGGA. These four sequences are used for reference since they have very different interactions with DB293 as can be seen in the figure. Equilibrium constants obtained from fitting results such as those in Figure 3, as described in Materials and Methods, are collected in Table 1.

*(A) Modifications at the G Base of -ATGA-*. Any change in G is of particular interest because it is unusual for a heterocyclic diamidine to bind strongly to GC base pairs in a minor groove complex. In fact, to our knowledge, DB293 is the first such compound to bind strongly to DNA sequences that contain GC base pairs, and it is the first dication of any type to form a stacked dimer in the minor groove. The sequences with G replaced by A, T, or C (Table 1) bind DB293 more weakly than the original ATGA. The sequence with G replaced by A, ATAA, would appear to be a classical AT minor groove binding sequence, but the results clearly show that it is not. This sequence, like ATGA, binds DB293 with positive cooperativity ($K_2 > K_1$) as a 2:1 complex. DB293 binds as a dimer to most, but not all, DNA sequences studied. The $K_1K_2$ value for the ATAA sequence is only about one-half that for ATGA. We have previously shown that the classical AATT sequence, used in many X-ray

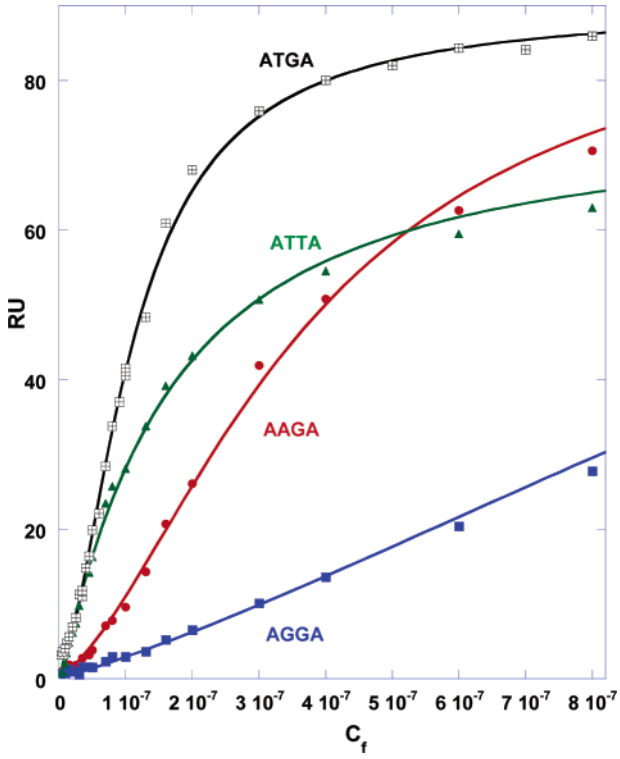


FIGURE 3: From sensorgrams such as those shown in Figure 2, the RU values at each free compound concentration were determined ($C_f$) and are plotted versus $C_f$ for the ATGA (open squares), AAGA (circles), ATTA (triangles), and AGGA (closed squares) sequences. Each DNA was immobilized through biotin−streptavidin capture, and experiments were conducted in MES10 buffer at 25 °C.

structural studies of minor groove binders, binds DB293 as a monomer (*29*).

The ATTA and ATCA sequences, with G mutations, bind DB293 with similar but somewhat lower equilibrium constants than with ATAA. The ATTA sequence, however,

binds DB293 in an importantly different way than with the other sequences in this set. The sequences with G, C, and A bind the compound with significant positive cooperativity ($K_2 > K_1$), but the sequence with a T does not ($K_2 < K_1$). As can be seen in Figure 3, the amount of DB293 bound to ATTA rises steeply at first and then more slowly. Fitting the results indicates that DB293 binds to ATTA as a dimer but with negative cooperativity in contrast to the positive cooperativity observed with the other sequences. It seems likely that the ATTA sequence is more similar to AATT and prefers binding a single DB293 in a narrow minor groove. This is the general type of binding expected for AT-specific minor groove dications, and it is the cooperative dimer that is quite unusual for diamidines.

*(B) Modifications at the T base of -ATGA-.* Replacement of the T with a G or C base creates a sequence with two adjacent GC base pairs and causes a drop in DB293 binding affinity. The sequence AGGA binds DB293 over 100 times more weakly than ATGA (Table 1). Although weak, the binding still appears cooperative (Figure 3). With ACGA the binding is reduced an additional factor of 3−4 and becomes difficult to quantitate. In this case, it is difficult to distinguish monomers and dimers because the $RU_{max}$ cannot be attained. Given the steric hindrance of the G-$NH_2$ group and third H-bond in the minor groove at GC base pairs, this reduction in binding is the expected result. Replacement of the T in ATGA with A causes a smaller, approximately 20-fold, reduction in binding compared to the DB293 complex with ATGA. This is a larger decrease than for any of the changes in replacement of the G of ATGA and illustrates the critical role that the GC in this sequence plays in specific recognition. The binding of DB293 to the AAGA sequence is cooperative and has a shape similar to that for DB293 binding to ATGA (Figure 3).

*DNase I Footprinting.* Initial footprinting experiments were performed with two 198-bp DNA restriction fragments, MS1 and MS2, containing the same sequence of 136 bp but cloned in the opposite orientation, 5′ → 3′ and 3′ → 5′. This so-called universal footprinting substrate (*36*) contains all 136 distinguishable tetranucleotide sequences [$(4^4)/2 + (4^{4/2})/2 = 136$] and represents therefore a very useful substrate to study the sequence selectivity of drugs such as DB293 with binding sites of 4 bp. The DNA substrates, 3′-end radiolabeled, were incubated with increasing concentrations of DB293 from 0.4 to 3 $\mu$M, and after equilibration, the complexes were subjected to limited cleavage by DNase I. The cleavage products were resolved by electrophoresis on sequencing gels. As shown in Figure 4, several footprints can be easily identified on the gels, reflecting binding of DB293 to specific sequences. At least five binding sites can be identified on each fragment. These sites were precisely located by densitometric analysis to provide the differential cleavage plots shown in Figure 5. From these graphs, both binding sequences (negative values) and nonbinding sequences (positive values) can be easily distinguished. The enhancement of DNase I cleavage at certain positions can be attributed to drug-induced local structural changes, which facilitates cutting by the enzyme at these sequences and/or redistribution of the enzymes (mass action effect), as previously discussed (*38*, *39*). Here, only the potential binding sites are considered.

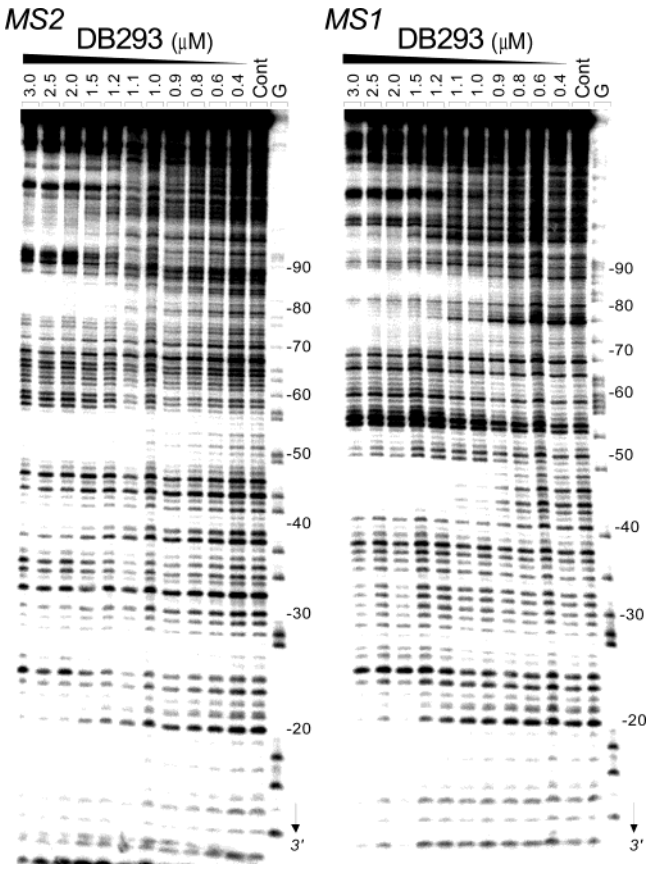


FIGURE 4: DNase I footprinting of DB293 on the *Hin*dIII−*Xba*I 198-bp MS1 and MS2 fragments containing the cloned sequence with a combination of all 136 distinguishable tetranucleotide sequences. In both cases, the DNA was 3′-end-labeled at the *Hin*dI site with [α-$^{32}$P]dATP in the presence of AMV reverse transcriptase. The products of nuclease digestion were resolved on an 8% polyacrylamide gel containing 8 M urea. The concentration ($\mu$M) of the drug is shown at the top of the appropriate gel lanes. Control tracks (Cont) contained no drug. The tracks labeled G represent dimethyl sulfate−piperidine markers specific for guanines. Numbers on the right side of the gel refer to the standard numbering scheme for the nucleotide sequence of the DNA fragments, as indicated in Figure 5.

From the differential cleavage plots, five footprints of variable intensity were located on fragment MS1, around nucleotide positions 21, 31, 44, 77, and 88, corresponding to the sequences 5′-TCTA, 5′-AATG, 5′-TCATCT, 5′-ATGT, and 5′-CGTG. With MS2, six sites can be identified around positions 21, 30, 40, 53, 70, and 82, corresponding to the sequences 5′-TCTA, 5′-ATAT, 5′-TGTATT, 5′-AATC, 5′-ACGA, and 5′-CCTTGATC. The first site, 5′-TAGA, common to MS1 and MS2, was found outside the cloned sequence. Three conclusions can be deduced from these data:

(i) The strongest site, clearly visible on MS1 around position 44 with 1 $\mu$M DB293, includes the sequence 5′-TCAT·5′-ATGA, which was previously identified as the most favorable binding site for this compound. The data obtained here with the "universal substrate" fully agree with our recent findings (*28*) and therefore tend to validate the information.

(ii) A number of DB293 binding sites contain four consecutive A·T base pairs, in particular, sequences ATAT, TATT, and AAAT (30, 40, and 53 on MS2). At first sight, binding to these sites may be attributed to the formation of classical 1:1 drug:DNA complexes with lower affinities

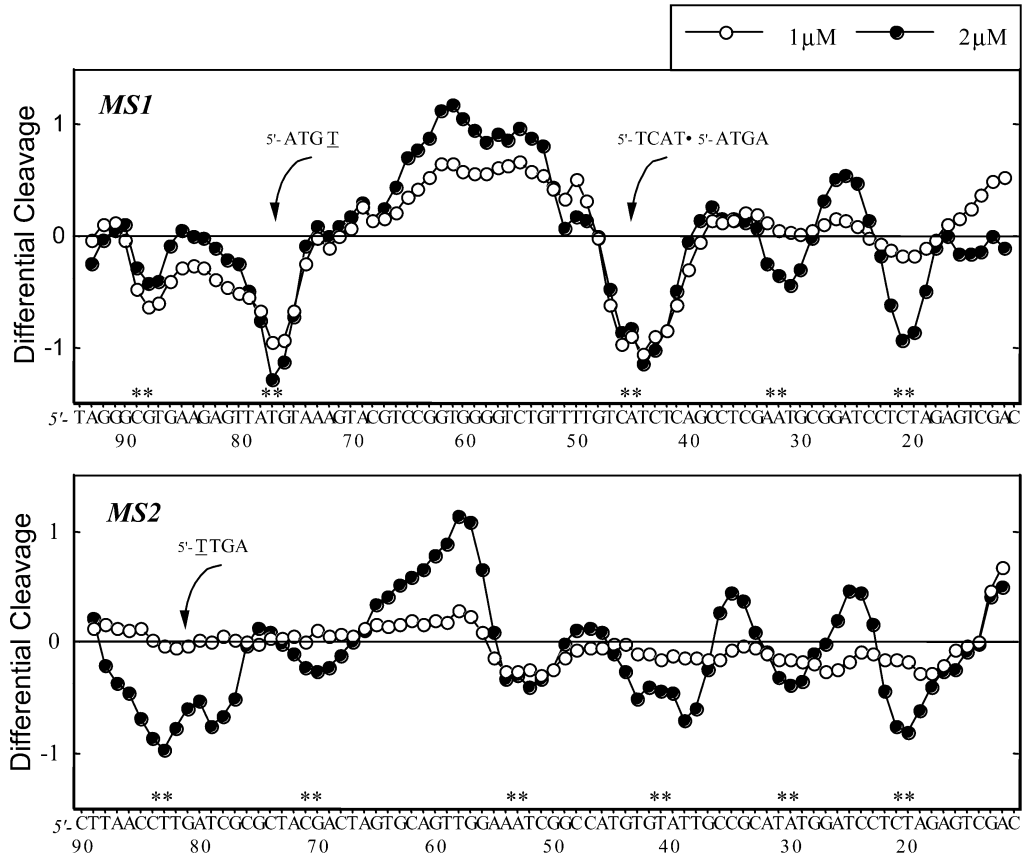


FIGURE 5: Differential cleavage plots comparing the susceptibility of the MS1 and MS2 fragments to DNase I cutting in the presence of DB293. Negative values correspond to a ligand-protected site, and positive values represent enhanced cleavage. Vertical scales are in units of $\ln f_a - \ln f_c$, where $f_a$ is the fractional cleavage at any bond in the presence of the drug and $f_c$ is the fractional cleavage of the same bond in the control, given closely similar extents of overall digestion. Only the region of the restriction fragment analyzed by densitometry is shown. The position of the footprints is indicated (**).

compared to the ATGA site. However, the above SPR data tell us that this conclusion may be too simple. Dimers can also form at AT sites, in particular, those including a TpA step, as observed by SPR with the ATAA sequence.

(iii) In addition, we found two sites corresponding to sequences where only one base (underlined) in the ATGA motif has been changed. DB293 tolerates sites TTGA (position 82 on MS2) and ATGT (position 77 on MS1), but given the intensity of the footprints, binding of DB293 to these two sites seems to be reduced by about 25% compared to what occurs at the ATGA. In terms of relative occupancy, the sites can be ranked in the order ATGA > ATGT > TTGA.

A weak site is also detected around the sequence TACGAC (position 77 on MS2), but a more detailed quantitative analysis (see below) indicates that the replacement of the central TG step by a CG dinucleotide is strongly disfavored, and this is consistent with the BIAcore experiments. The weak footprint seen on fragment MS2 is likely due to the flanking AC and CA steps.

On the basis of these observations, we went on cloning duplexes A and B containing selected variants of the ATGA motif. After cloning, two restriction fragments of 319 bp in length were prepared, 3′-end radiolabeled, and used in quantitative footprinting experiments with a large range of concentrations of DB293. For each fragment, the experimental conditions were optimized in preliminary experiments to find the appropriate drug and enzyme concentrations and reaction time. An example of a gel obtained with duplex B is shown in Figure 6. On the gel, seven footprints can be visualized and reflect preferential interaction of DB293 with specific sequences. Even before the densitometric analysis was carried out, it is already clear at this point that the digestion by the nuclease is not inhibited to the same extent at different sites. For example, the footprint around position 35 occurs for drug concentrations >2 $\mu$M whereas that at position 55 is already pronounced at 1 $\mu$M. Depending on the affinity of DB293 for one site or another, the enzyme activity is differently attenuated, providing thus a useful tool to differentiate between these sites.

A full densitometric analysis of the gels was performed, not only to locate the binding sites but also to estimate the drug concentration required for half-maximal footprinting, named $C_{50}$ values. Under the conditions of the footprinting experiments a large fraction of the ligand must be free, so that these $C_{50}$ values may approximate to dissociation constants for binding to individual sites. The analysis was limited to the regions where the DNA bands are sufficiently well resolved to permit unambiguous analysis, but given the good resolution of the gels, about 80 bands (nucleotides) were quantified on each fragment. Still, the sequence of a few sites, such as those corresponding to the black boxes in Figure 6, could not be precisely identified and therefore were not considered for the analysis. But all duplex A and B sequences were analyzed. The differential cleavage plots are shown in Figure 7. In both cases, only the radiolabeled strand

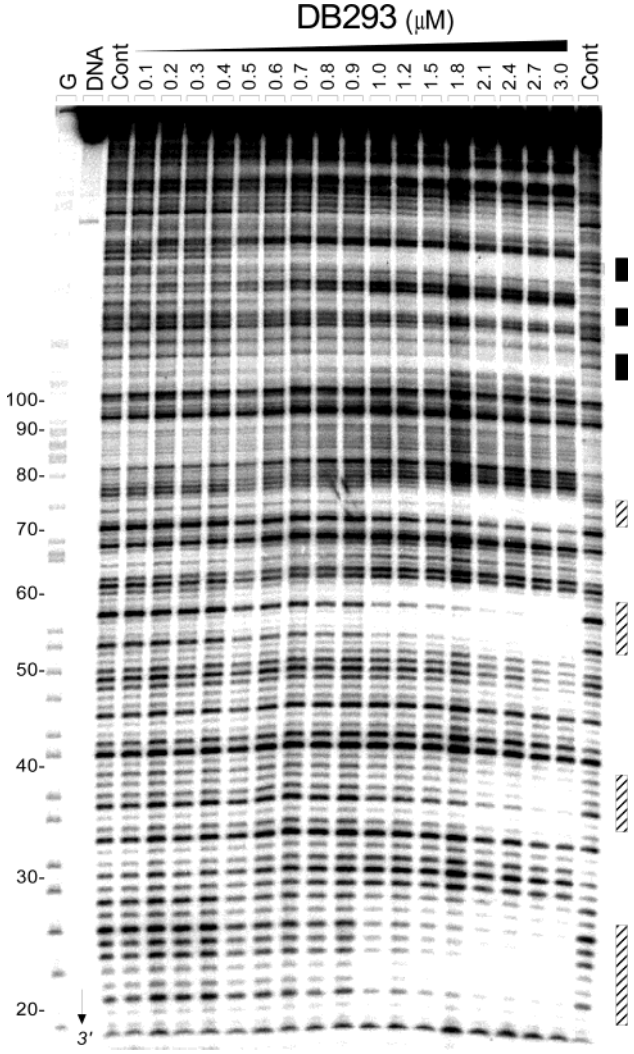


FIGURE 6: DNase I footprinting of DB293 on the 319-bp fragment containing cloned duplex B. Numbers on the left side of the gel refer to the standard numbering scheme for the nucleotide sequence of the DNA fragment, as indicated in Figure 7. The vertical boxes indicate the positions of inhibition of DNase I cutting in the presence of the drugs. Other details as for Figure 4. The three sites at the top of the gels (filled bars) could not be quantified. The densitometric analysis covered the four lower sites (hatched bars).

of the duplex in indicated. The targeted tetranucleotide sequences (underlined by thick bars) are separated by an "insulator" sequence (underlined by dashed lines) to which the compound should not bind. On the basis of our previous footprinting studies (*28*, *29*), it was predicted that this specific sequence, 5′-AGCAAGCG, should not correspond to any type of binding site for DB293, be it a 1:1 or a 2:1 site. The results show that this nonbinding sequence was correctly chosen because in all cases, but one, the observed footprints coincide with the position of the targeted tetranucleotide but not the insulator sequence. There is, however, one case where a footprint includes a portion of this insulator sequence, between positions 53 and 58 on duplex B. The absence of two bases, AG, on the 5′ side disrupts the isolation potential of the sequence, and a strong footprint corresponding to the sequence ACAA is observed. But apart from this isolated case, the results attest that the design of the DNA fragments was correct.

On both fragments A and B, the common sequence 5′-TCAT·5′-ATGA around position 15 corresponds to a high-affinity site for DB293, showing once again that this tetranucleotide indeed represents a preferential target for the drug. But apart from this primary site, it is clear that the drug can also interact with a number of secondary sites which sequences differ for 1 or 2 bases from the ATGA site. With this footprinting approach, it is not possible to clone all potential tetranucleotide sites as studied in the SPR experiments. But at least a few sites can be designed and tested simultaneously for binding to DB293. We have limited our selection of sites to a few modifications, in particular, to test the importance of the only G·C base pair in the ATGA motif. The underlined cytosine of TCAT was replaced with a thymine (TTAT) or a guanine (TGAT). The second category of potential sites tested corresponds to sequences for which the central CA dinucleotide (TCAT) was inverted (TACT), translated (TTGT, pyrimidine C → T, purine A → G), or replaced with two G·C base pairs (TGCT). For each site, the $C_{50}$ value was determined from the corresponding cleavage plot, as shown in Figure 8. In these graphs, the relative cleavage intensity $R$ is plotted as a function of the total ligand concentration. A $C_{50}$ value of 1.2 $\mu$M was measured for the primary site TCAT. The $C_{50}$ values are about 2-fold and 3-fold higher when the C is replaced by a T ($C_{50}$ = 2.5 $\mu$M for TTAT) and a G ($C_{50} \sim$ 3.5 $\mu$M for TGAT), respectively (Figure 8A). With regard to the sites where the two central bases have been mutated (Figure 8B), the following results were obtained:

(i) The substitution of TTGT for TCAT does not reduce the relative affinity of DB293 for its target. In contrast, the binding may be reinforced because the $C_{50}$ value is slightly decreased (from 1.2 to 0.9 $\mu$M ± 0.06). In other words, the translation of the pyrimidine−purine doublet by the opposite pairs maintains a high-affinity site for the drug.

(ii) On the opposite, the TCAT → TAGT substitution reduces significantly the drug affinity ($C_{50} >$ 3 $\mu$M).

(iii) The most pronounced modification was observed when the TCAT was replaced with a TCGT sequence. DB293 completely fails to protect this CG site from DNase I cleavage. This is in perfect agreement with the SPR data indicating a 500-fold decrease of affinity with this sequence (Table 1).

The binding site around position 58 on duplex B corresponds to the sequence ACAA. It is interesting to note that the affinity of DB293 for this site is superior to that of site TCAT (Figure 8C). This observation is consistent with the previous data showing that DB293 binds less strongly to 5′-TCAT compared to 5′-TTGT. Therefore, the analysis of two different sites with complementary sequences, 5′-TTGT and 5′-ACAA, provides consistent data that identify this sequence as another privileged binding site for DB293.

The mutation of the adenine residue of TCAT into a guanine totally inhibits binding of the drug. As shown in Figure 8D, DNase I cleavage at 5′-TCGT is not inhibited but in contrast strongly enhanced. A binding site was also identified outside the insert sequence, around nucleotide positions 70−76. This site provides interesting information because it encompasses the sequence 5′-TAGA. The inversion of the first two A·T pairs (5′-TCAT → 5′-TCTA) reduces significantly binding of DB293. DNase I cleavage at 5′-TCTA cannot be reduced by more than 45% even in the presence of a high drug concentration (Figure 8E). Finally, the last site identified in duplex B corresponds to

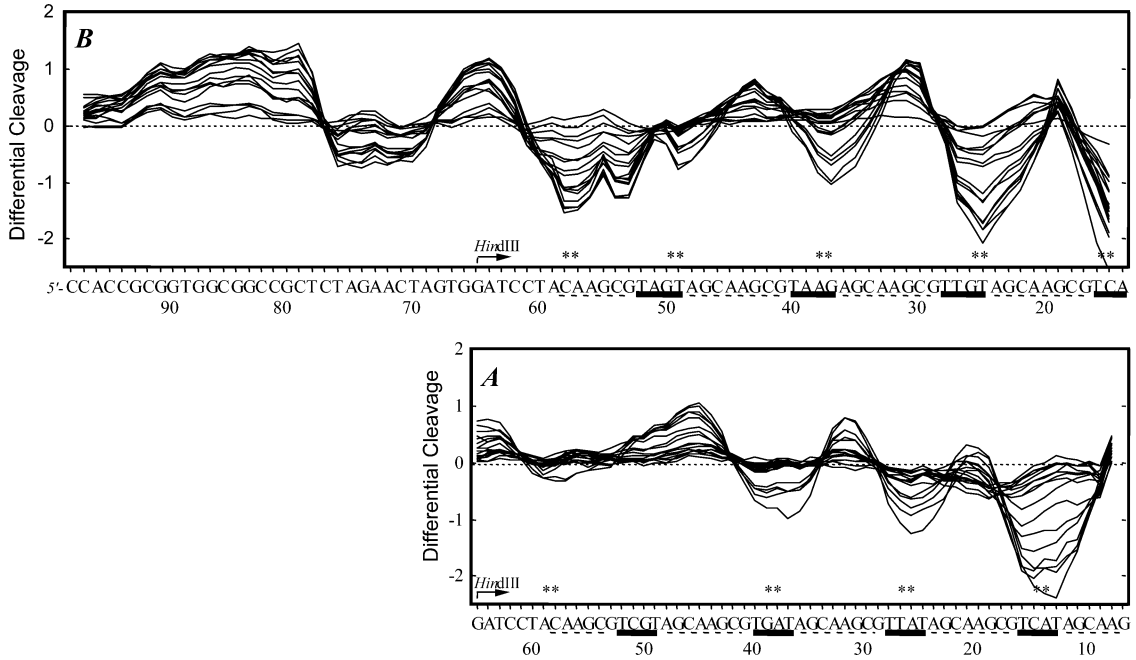


FIGURE 7: Differential cleavage plots comparing the susceptibility of DNA duplexes A and B to DNase I cutting in the presence of increasing concentrations of DB293 (0.1−3 $\mu$M; top to bottom curves at position 25). Other details as for Figure 5 and in the text.

the sequence 5′-AAGA around position 38. Again, we observe that the 5′-ATGA → 5′-AAGA substitution reduced considerably binding of DB293 to DNA (Figure 8F).

## DISCUSSION

The rational design of DNA minor groove binders to "on demand" manipulate gene expression remains tantalizing, but uncertain. Promising results have been reported with hairpin polyamides to disrupt gene expression at the level of transcription (*6*, *10*, *40*, *41*). But if the concept of turning on/off the expression of specific genes implicated in specific diseases, cancer progression for example, is very elegant, such a gene-targeted approach is still in its infancy and the therapeutic benefits are far from being realized. It is essential to fully elucidate the molecular rules used by these minor groove binders to read the genetic information to be able to manipulate them to tune the activity of specific genes (*42*). It is especially important to use cell-permeable molecules such as DB293 (*43*), which have significant therapeutic potential, for such studies.

Three main classes of DNA minor groove binders are actively studied. In terms of DNA sequence recognition, there is no doubt that the hairpin polyamides, derived from the antibiotics netropsin and distamycin, represent the best developed box of tools to chemically achieve gene knockout. The utility of these tools as therapeutic agents, however, is perhaps overestimated, at least until the issue of limited nuclear uptake can be solved. Bis(benzimidazole) molecules, issued from the dye Hoechst 33258, form another class of DNA-reading molecules. These compounds are also very attractive for several reasons, including (i) the capacity to form 2:1 complexes for a more sequence-specific DNA recognition (*44*−*46*), (ii) the possibility to achieve a high degree of selectivity through the targeting of long DNA sequences, up to a complete helical turn (*47*), and, above all, (iii) their anticancer potential. Several types of bis(benzimidazole) derivatives exert potent cytotoxic activities, and in some cases this is linked to topoisomerase I inhibition (*48*, *49*). The third class of compounds are the diamidine derivatives related to furamidine which have emerged over the past 10 years as a very promising series of nonpeptidic DNA minor groove binders. These unfused aromatic dications easily enter into cells and accumulate in cell nuclei (*43*). Recent experiments indicated that binding to DNA provides the main driving force attracting the compounds into the cell nucleus (*50*). Although furamidine derivatives are primarily developed as antiparasitic agents, some studies suggest that this family of drugs might also be useful in the treatment of cancer (*51*).

A recent body of work has focused on designing furamidine analogues capable of recognizing not only AT sites but also more specific sequences containing G·C base pairs. Significant progress has been made in identifying DB293 as a lead candidate for gene targeting. This dication, which only differs from furamidine by the substitution of a benzimidazole for a phenyl ring, strongly binds to DNA with a preference for ATGA sequences. The present study confirms that this motif is a high-affinity receptor site for DB293, and the systematic substitution of its second or third base provides clear evidence for the essential role of the central TG step. The key feature of the ATGA−DB293 interaction is positive cooperativity, which reflects the insertion of a drug dimer within the minor groove. All modifications of the central TG step have resulted in a drop of the binding constant (compare the $K_1K_2$ products for the different sequences listed in Table 1). The second base pair in ATGA seems to dominate the interaction. The replacement of the T by a C decreases the binding affinity by a factor of more than 500 whereas the replacement of the third base G by a T, C, or A only decreases the affinity by a factor of 4 at most. According to the SPR experiments, the dinucleotide CG shows little or no interaction with DB293. It is therefore not surprising to observe that this dinucleotide is well

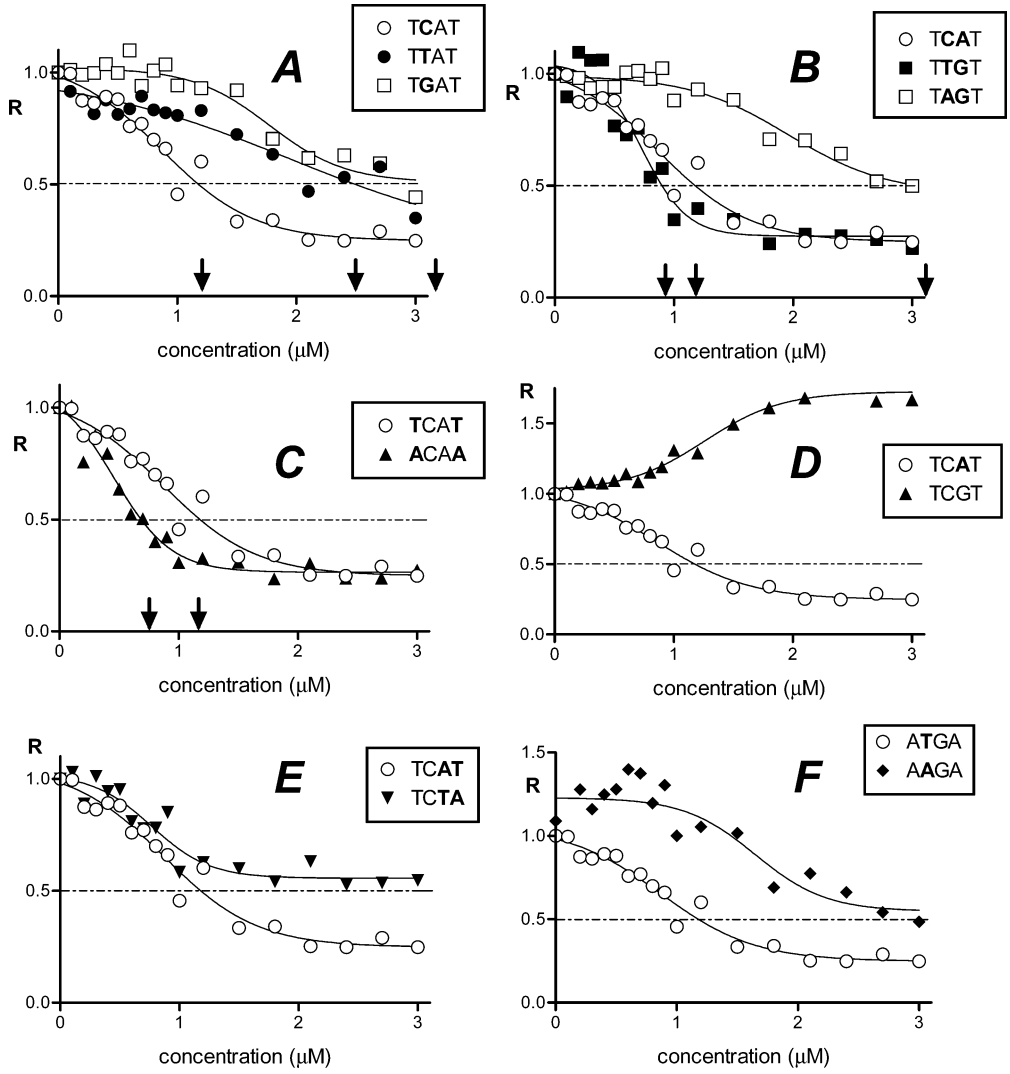


FIGURE 8: Footprinting plots for the binding of DB293 to different sites. The relative band intensity $R$ corresponds to the ratio $I_c/I_0$, where $I_c$ is the intensity of the band at the ligand concentration $c$ and $I_0$ is the intensity of the same band in the absence of DB293. These graphs were used to determine the $C_{50}$ values for half-maximal footprinting.

represented in the insulator sequence 5′-AGCAAGCG used to separate the binding sites in the restriction fragment used for the footprinting experiments. The central TG step of ATGA is well adapted to accommodate the DB293 dimer. The T → A and G → C substitutions decrease affinity by factors of 23 and 4, respectively, but when these two base pair inversions are made simultaneously, i.e., ATGA → AACA, the drug interaction remains essentially unaffected, as judged from the footprinting results.

The diagram in Figure 9a summarizes the footprinting data. In most cases, the mutation of the primary site 5′-ATGA·5′-TCAT reduces the strength of binding of DB293 to the target sequence. The mutation can also be very detrimental, as is the case when two adjacent G·C base pairs are incorporated. The drug can interact with a central TpG or GpA step but not with a central GpC or CpG dinucleotide. Interestingly, a new high-affinity binding site has been identified: 5′-ACAA·5′-TGTT. Collectively, the SPR and footprinting data allow us to define a consensus sequence for the cooperative 2:1 binding of DB293 to DNA: 5′-(A/T)-TG-(A/T) (Figure 9b). As mentioned above, the (A)-TG-(A) and (T)-TG-(T) provide slightly better binding sites than the asymmetric (A)-TG-(T) and (T)-TG-(A) sequences. Substitution of the central dinucleotide has a profound impact on drug binding. As schematized in Figure 9c, the central dinucleotides can be grouped in three categories: the high-affinity sites (TG and CA), the reduced affinity sites (AG, GA, TC, and CT), and the excluded sites (CG and GC).

Another important point to mention is the facile cooperativity for the binding of DB293 to its target sequence. The T → A, C, G or G → A, T, C substitutions in ATGA all reduce significantly the extent of drug binding, but generally these substitutions do not prevent the cooperativity. The only case where the positive cooperativity seen upon binding of DB293 to ATGA is lost is with the motif ATTA. Symmetric A/T-containing tetrads such as AATT and ATTA form very strong monomer complexes and cannot readily accommodate a dimer of DB293. In general, as previously observed with related compounds in the diphenylfuran series (*52*), these diamidines bind well to $(A/T)_4$ sites, but they prefer AATT compared to TTAA due to the unusual structure generated by TpA dinucleotides. A TpA step inserted into an A-tract has the effect of widening the minor groove and disrupting the single-file hydration motif (*53*). $d(TTAA)_2$ tracts are associated with wider minor grooves than $d(AATT)_2$ seg-

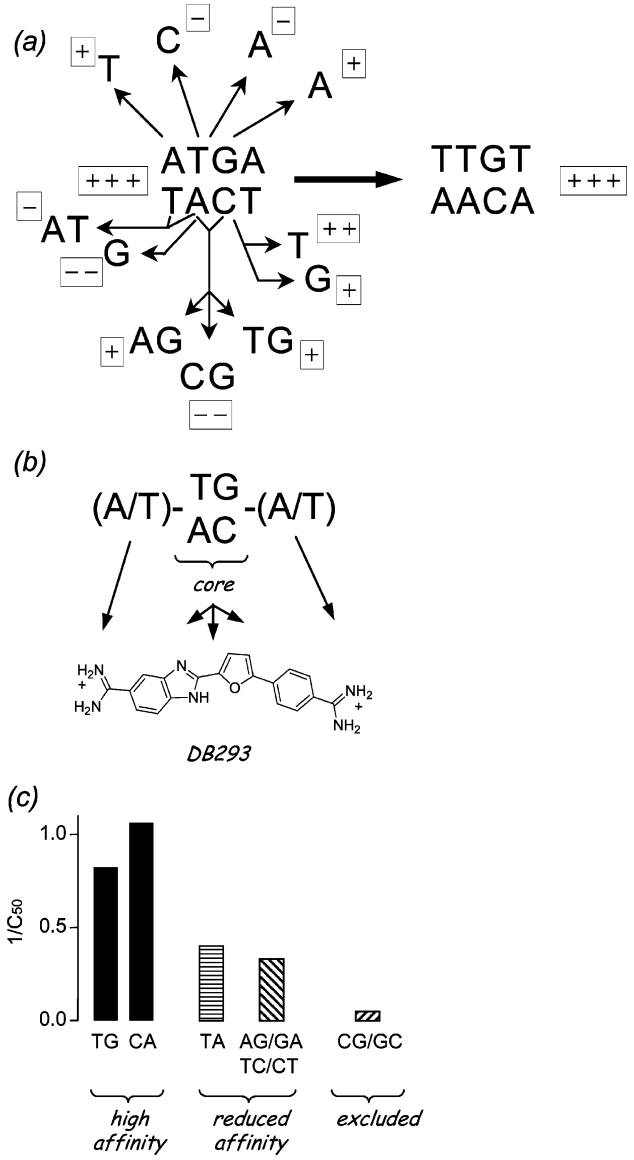


FIGURE 9: (a) Summary map for the footprinting data. Symbols +++, ++, and + refer to sites of high, medium, and low affinity, respectively. The (−) symbol indicates little or no binding to this sequence. (b) Consensus sequence for the binding of DB293 to DNA. The external AT bp is recognized by the amidine functions of DB293 while its phenylfuran−benzimidazole (dimerized) core is responsible for the recognition of the central TG unit. (c) Influence of the central dinucleotide on drug binding. The histogram shows the variation of the $1/C_{50}$ values (taken from the footprinting data) with the nature of the central dinucleotide.

ments and a disordered hydration pattern in their minor grooves (*54*). The other tetranucleotide combinations tested, including low-affinity sites such as AGGA and ACGA, however, all show positive cooperativity, suggesting that drug dimers can preferentially form at these sites. This reflects the high capacity of DB293 molecules to stack in a DNA-directed manner. Cooperative dimerization of DB293 is not restricted to the few sites of very high affinity but can apparently occur at a number of cognate sites, suggesting that the stacked arrangement represented a favored conformation for the drug. The high tendency of DB293 to bind DNA in a cooperative process is unique for dications and is an important new concept in the design of cell-permeable agents with gene regulatory potential.

## REFERENCES


1. Bailly, C., and Chaires, J. B. (1998) Design of sequence-specific DNA minor groove binders. Netropsin and distamycin analogues, *Bioconjugate Chem. 9*, 513−538.
2. Neidle, S. (2001) DNA minor-groove recognition by small molecules, *Nat. Prod. Rep. 18*, 291−309.
3. Lown, J. W. (1995) Design and development of sequence-selective lexitropsin DNA minor groove binders, *Drug Dev. Res. 34*, 145−183.
4. Dervan, P. B., and Bürli, R. W. (1999) Sequence-specific DNA recognition by polyamides, *Curr. Opin. Chem. Biol. 3*, 688−693.
5. Dervan, P. B. (2001) Molecular recognition of DNA by small molecules, *Bioorg. Med. Chem. 9*, 2215−2235.
6. Gottesfeld, J. M., Turner, J. M., and Dervan, P. B. (2000) Chemical approaches to control gene expression, *Gene Expression 9*, 77−91.
7. Mapp, A. K., Ansari, A. Z., Ptashne, M., and Dervan, P. B. (2000) Activation of gene expression by small molecule transcription factors, *Proc. Natl. Acad. Sci. U.S.A. 97*, 3930−3935.
8. Janssen, S., Cuvier, O., Muller, M., and Laemmli, U.K. (2000) Specific gain- and loss-of-function phenotypes induced by satellite-specific DNA-binding drugs fed to *Drosophila melanogaster*, *Mol. Cell 6*, 1013−1024.
9. Gottesfeld, J. M., Neely, L., Trauger, J. W., Baird, E. E., and Dervan, P. B. (1997) Regulation of gene expression by small molecules, *Nature 387*, 202−205.
10. Ehley, J. A., Melander, C., Herman, D., Baird, E. E., Ferguson, H. A., Goodrich, J. A., Dervan, P. B., and Gottesfeld, J. M. (2002) Promoter scanning for transcription inhibition with DNA-binding polyamides, *Mol. Cell. Biol. 22*, 1723−1733.
11. Sharma, S. K., Morrissey, A. T., Miller, G. G., Gmeiner, W. H., and Lown, J. W. (2001) Design, synthesis, and intracellular localization of a fluorescently labeled DNA binding polyamide related to the antibiotic distamycin, *Bioorg. Med. Chem. Lett. 11*, 769−772.
12. Belitsky, J. M., Leslie, S. J., Arora, P. S., Beerman, T. A., and Dervan, P. B. (2002) Cellular uptake of *N*-methylpyrrole/*N*-methylimidazole polyamide-dye conjugates, *Bioorg. Med. Chem. 10*, 3313−3318.
13. Tidwell, R. R., and Boykin, D. W. (2003) Dicationic DNA minor groove binders as antimicrobial agents, in *DNA and RNA Binders* (Demeunynck, M., Bailly, C., and Wilson, W. D., Eds.) pp 414−460, Wiley-VCH, New York.
14. Boykin, D. W., Kumar, A., Spychala, J., Zhou, M., Lombardi, R. L., Wilson, W. D., Dykstra, C. C., Jones, S. K., Hall, J. E., Tidwell, R. R., Laughton, C., Nunn, C. M., and Neidle, S. (1995) Dicationic diarylfurans as anti-*Pneumocystis carinii* agents, *J. Med. Chem. 38*, 912−916.
15. Boykin, D. W., Kumar, A., Xiao, G., Wilson, W. D., Bender, B. C., McCurdy, D. R., Hall, J. E., and Tidwell, R. R. (1998) 2,5-bis[4-*N*-alkylamidino)phenyl]furans as anti-*Pneumocystis carinii* agents, *J. Med. Chem. 41*, 124−129.
16. Hopkins, K. T., Wilson, W. D., Bender, B. C., McCurdy, D. R., Hall, J. E., Tidwell, R. R., Kumar, A., Bajic, M., and Boykin, D. W. (1998) Extended aromatic furan amidino derivatives as anti-*Pneumocystis carinii* agents, *J. Med. Chem. 41*, 3872−3878.
17. Francesconi, I., Wilson, W. D., Tanious, F. A., Hall, J. E., Bender, B. C., Tidwell, R. R., McCurdy, D., and Boykin, D. W. (1999) 2,4-Diphenyl furan diamidines as novel anti-*Pneumocystis carinii* pneumonia agents, *J. Med. Chem. 42*, 2260−2265.
18. Rahmathullah, S. M., Hall, J. E., Bender, B. C., McCurdy, D. R., Tidwell, R. R., and Boykin, D. W. (1999) Prodrugs of amidines: synthesis and anti-*Pneumocystis carinii* activity of carbamates of 2,5-bis(4-amidinophenyl)furan, *J. Med. Chem. 42*, 3994−4000.
19. Das, B. P., and Boykin, D. W. (1977) Synthesis and antiprotozoal activity of 2,5-bis(4-guanylphenyl)furans, *J. Med. Chem. 20*, 531−536.
20. Blagburn, B. L., Drain, K. L., Land, T. M., Moore, P. H., Lindsay, D. S., Kumar, A. J., Shi, J., Boykin, D. W., and Tidwell, R. R. (1998) Dicationic furans inhibit development of Cryptosporidium Parvum in HSD/ICR suckling mice, *J. Parasitol. 84*, 851−856.
21. Stephens, C. E., Tanious, F., Kim, S., Wilson, W. D., Schell, W. A., Perfect, J. R., Franzblau, S. G., and Boykin, D. W. (2001) Diguanidino and "reversed" diamidino 2,5-diarylfurans as antimicrobial agents, *J. Med. Chem. 44*, 1741−1748.

22. Boykin, D. W., Kumar, A., Bender, B. K., Hall, J. E., and Tidwell, R. R. (1996) Anti-*Pneumocystis* activity of bis-amidoximes and bis-*O*-alkylamidoximes prodrugs, *Bioorg. Med. Chem. Lett. 6*, 3017−3020.
23. Dykstra, C. C., McClernon, D. R., Elwell, L. P., and Tidwell, R. R. (1994) Selective inhibition of topoisomerases from *Pneumocystis carinii* compared with that of topoisomerases from mammalian cells, *Antimicrob. Agents Chemother. 38*, 1890−1898.
24. Hildebrandt, E., Boykin, D. W., Kumar, A., Tidwell, R. R., and Dystra, C. C. (1998) Identification and characterization of an endo/exonuclease in *Pneumocystis carinii* that is inhibited by dicationic diarylfurans with efficacy against *Pneumocystis pneumonia*, *J. Eukaryotic Microbiol. 45*, 112−121.
25. Wang, L., Bailly, C., Kumar, A., Ding, D., Bajic, M., Boykin, D. W., and Wilson, W. D. (2000) Specific molecular recognition of mixed nucleic acid sequences: An aromatic dication that binds in the DNA minor groove as a dimer, *Proc. Natl. Acad. Sci. U.S.A. 97*, 12−16.
26. Pelton, J. G., and Wemmer, D. E. (1990) Binding modes of distamycin A with d(CGCAAATTTGCG)$_2$ determined by two-dimensional NMR, *J. Am. Chem. Soc. 112*, 1393−1399.
27. Pelton, J. G., and Wemmer, D. E. (1989) Structural characterization of a 2:1 distamycin A·d(CGCAAATTGGC) complex by two-dimensional NMR, *Proc. Natl. Acad. Sci. U.S.A. 86*, 5723−5727.
28. Bailly, C. Tardy, C., Wang, L., Armitage, B., Hopkins, K., Kumar, A., Schuster, G. B., Boykin, D. W., and Wilson, W. D. (2001) Recognition of ATGA sequences by the unfused aromatic dication DB293 forming stacked dimers in the DNA minor groove, *Biochemistry 40*, 9770−9779.
29. Wang, L., Carrasco, C., Kumar, A., Stephens, C. E., Bailly, C., Boykin, D. W., and Wilson, W. D. (2001) Evaluation of the influence of compound structure on stacked-dimer formation in the DNA minor groove, *Biochemistry 40*, 2511−2521.
30. Wang, L., Kumar, A., Boykin, D. W., Bailly, C., and Wilson, W. D. (2002) Comparative thermodynamics for monomer and dimer sequence-dependent binding of a heterocyclic dication in the DNA minor groove, *J. Mol. Biol. 317*, 361−374.
31. Wilson, W. D. (2002) Analyzing biomolecular interactions, *Science 295*, 2103−2105.
32. Trauger, J. W., and Dervan, P. B. (2001) Footprinting methods for analysis of pyrrole-imidazole polyamide/DNA complexes, *Methods Enzymol. 340*, 450−466.
33. Fox, K. R., and Waring, M. J. (2001) High-resolution footprinting studies of drug−DNA complexes using chemical and enzymic probes, *Methods Enzymol. 340*, 412−430.
34. Wilson, W. D., Wang, L., Tanious, F., Kumar, A., Boykin, D. W., Carrasco, C., and Bailly, C. (2001) BIAcore and DNA footprinting for discovery and development of new DNA targeted therapeutics and reagents, *BIAcore J. 1*, 15−19.
35. Davis, T. M., and Wilson, W. D. (2000) Determination of the refractive index increments of small molecules for correction of surface plasmon resonance data, *Anal. Biochem. 284*, 348−353.
36. Lavesa, M., and Fox, K. R. (2001) Preferred binding sites for [N-MeCYs(3), N.-MeCys(7)]TANDEM determined using a universal footprinting substrate, *Anal. Biochem. 293*, 246−250.
37. Bailly, C., and Waring, M. J. (1995) Comparison of different footprinting methodologies for detecting binding sites for a small ligand on DNA, *J. Biomol. Struct. Dyn. 12*, 869−898.
38. Goodisman, J., and Dabrowiak, J. C. (1992) Structural changes and enhancements in DNase I footprinting experiments, *Biochemistry 31*, 1058−1064.
39. Bailly, C., Hamy, F., and Waring, M. J. (1996) Cooperativity in the binding of echinomycin to DNA fragments containing closely spaced CpG sites, *Biochemistry 35*, 1150−1161.
40. Gottesfeld, J. M., Belitsky, J. M., Melander, C., Dervan, P. B., and Luger, K. (2002) Blocking transcription through a nucleosome with synthetic DNA ligands, *J. Mol. Biol. 321*, 249−263.
41. Wurtz, N. R., Pomerantz, J. L., Baltimore, D., and Dervan, P. B. (2002) Inhibition of DNA binding by NF-kappa B with pyrrole-imidazole polyamides, *Biochemistry 41*, 7604−7609.
42. Lacy, E. R., Madsen, E. M., Lee, M., and Wilson, W. D. (2003) Polyamide dimer stacking in the DNA minor groove and recognition of T·G mismatched base pairs in DNA, in *Small Molecule DNA and RNA Binders* (Demeunynck, M., Bailly, C., and Wilson, W. D., Eds.) Vol. 2, pp 384−413, Wiley-VCH, New York.
43. Lansiaux, A., Dassonneville, L., Facompre, M., Kumar, A., Stephens, C. E., Bajic, M., Tanious, F., Wilson, W. D., Boykin, D. W., and Bailly, C. (2002) Distribution of furamidine analogues in tumor cells: influence of the number of positive charges, *J. Med. Chem. 45*, 1994−2002.
44. Browne, K. A., He, G.-X., and Bruice, T. C. (1993) Microgonotropens and their interactions with DNA. 2. Quantitative evaluation of equilibrium constants for 1:1 and 2:1 binding of dien-microgonotropen-a, -b, and -c as well as distamycin and Hoechst 33258, *J. Am. Chem. Soc. 115*, 7072−7079.
45. Satz, A. L., White, C. M., Beerman, T. A., and Bruice, T. C. (2001) Double-stranded DNA binding characteristics and subcellular distribution of a minor groove binding diphenyl ether bisbenzimidazole, *Biochemistry 40*, 6465−6474.
46. Mazur, S., Tanious, F. A., Ding, D., Kumar, A., Boykin, D. W., Simpson, I. J., Neidle, S., and Wilson, W. D. (2000) A thermodynamic and structural analysis of DNA minor groove complex formation, *J. Mol. Biol. 300*, 321−337.
47. Joubert, A., Sun, X.-W., Johansson, E., Bailly, C., Mann, J., and Neidle, S. (2003) Sequence selective targeting of long stretches of the DNA minor groove by a novel dimeric bis-benzimidazole, *Biochemistry 42*, 5984−5992.
48. Xu, Z., Li, T.-K., Kim, J. S., LaVoie, E., Breslauer, K. J., Liu, L. F., and Pilch, D. S. (1998) DNA minor groove binding-directed poisoning of human DNA topoisomerase I by terbenzimidazoles, *Biochemistry 37*, 3558−3566.
49. Jin, S., Kim, J. S., Sim, S.-P., Liu, A., Pilch, D. S., Liu, L. F., and LaVoie, E. J. (2000) Heterocyclic bibenzimidazole derivatives as topoisomerase I inhibitors, *Bioorg. Med. Chem. Lett. 10*, 719−723.
50. Lansiaux, A., Tanious, F., Mishal, Z., Dassonneville, L., Kumar, A., Stephens, C. E., Hu, O., Wilson, W. D., Boykin, D. W., and Bailly, C. (2002) Distribution of furamidine analogues in tumor cells: Targeting of the nucleus or mitochondria depending on the amidine substitution, *Cancer Res. 62*, 7219−7229.
51. Neidle, S., Kelland, L. R., Trent, J. O., Simpson, I. J., Boykin, D. W., Kumar, A., and Wilson, W. D. (1997) Cytotoxicity of bis-(phenylamidinium)furan alkyl derivatives in human tumour cell lines: Relation to DNA minor groove binding, *Bioorg. Med. Chem. 7*, 1403−1408.
52. Nguyen, B., Tardy, C., Bailly, C., Colson, P., Houssier, C., Kumar, A., Boykin, D. W., and Wilson, W. D. (2002) Influence of compound structure on affinity, sequence selectivity and mode of binding to DNA for unfused aromatic dications related to furamidine, *Biopolymers 63*, 281−297.
53. Quintana, J. R., Grzeskowiak, K., Yanagi, K., and Dickerson, R. E. (1992) Structure of a B-DNA decamer with a central T-A step: C-G-A-T-T-A-A-T-C-G, *J. Mol. Biol. 225*, 379−385.
54. Liepinsh, E., Leupin, W., and Otting, G. (1994) Hydration of DNA in aqueous solution: NMR evidence for a kinetic destabilization of the minor grove hydration of d-(TTAA)$_2$ versus d-(AATT)$_2$ segments, *Nucleic Acids Res. 22*, 2249−2254.

BI034852Y